Activation–relaxation processes and related effects in quantum conductance of molecular junctions

OPEN ACCESS
IOP Publishing
Nanotechnology

Nanotechnology **31** (2020) 045001 (7pp)
https://doi.org/10.1088/1361-6528/ab4d96

Activation–relaxation processes and related effects in quantum conductance of molecular junctions

F Gasparyan[1,2], **N Boichuk**[1] **and S Vitusevich**[1]

[1] Bioelectronics (ICS-8), Forschungszentrum Jülich, D-52425, Jülich, Germany
[2] Yerevan State University, 1 Alex Manoogian St., 0025, Yerevan, Armenia

E-mail: S.Vitusevich@fz-juelich.de

Received 26 April 2019, revised 2 August 2019
Accepted for publication 14 October 2019
Published 30 October 2019

Abstract

We reveal the comparative relationship between small changes in quantum conductivity behavior for molecular junctions. We clarify the mechanisms of acquiring and losing additional thermal activation energy during average current flow in a gold-1,4 benzenediamine (BDA)-gold molecular junction and explain the quantum conductance modulation process. Small changes in working temperature lead to a change in quantum conductivity, which is reflected in random telegraph signal behavior. We demonstrate the high sensitivity of the BDA molecules to small changes in temperature. For BDA molecules, conductance thermo-sensitivity values are relatively high near to $(0.8 \div 1.6) \times 10^{-7}\ \Omega^{-1}\ K^{-1}$. This advantage can be used to measure weak variations in the ambient temperature. We show that the additional thermal energy arising from the change in temperature can impact on the strength of the electrode-molecule coupling, on the modulation of quantum conductivity. Local changes in quantum conductance of the order of quanta or smaller are conditioned by small random changes in the working regime arising from some of the activation processes. On the basis of the modulation of conductance, we calculate the magnitude of the spring constant of the 1,4 benzenediamine molecule as $k_s \approx 7.1 \times 10^{-3}\ N\ m^{-1}$ at the stretching length of 0.03 nm for the Au−NH_2 molecular junction.

Keywords: quantum conductance, molecular junction, random telegraph signal

(Some figures may appear in colour only in the online journal)

1. Introduction

Charge transport through organic molecular junctions has been widely investigated in the past. In general, researchers are focused on a detailed theoretical and experimental study of transport mechanisms through several organic molecules. They look at the peculiarities of the energy band structure between the highest occupied molecular orbital (HOMO) and the lowest unoccupied molecular orbital (LUMO) of metal–molecule–metal junctions [1–21]. It is well known that transport characteristics are determined by the intrinsic properties of the molecules, such as their length, conformation and orientation, the gap between the HOMO and the LUMO, and the alignment of this gap to the metal Fermi level. Electrical transport through the molecular model systems benzenediamine, benzenedithiol, hexanedithiol and hexanediamine was investigated in detail in [4, 20]. Conductance histograms under different experimental conditions indicate that measurements using the mechanically controllable break junction (MCBJ) technique in vacuum are limited by the surface density of molecules at the contact. For both benzenediamine and benzenedithiol, a large variability in low-bias conductance was observed in the experiment [4]. Authors of [4] attribute this variability to the slow breaking of the lithographically processed MCBJs. The low-bias conductance of a series of substituted 1.4-benzenediamine (BDA)

molecules was measured while breaking a gold point contact in a solution of the molecules in [18]. A conductance value of BDA in a lower current range was found in [22]. The conductance of individual BDA-Au molecular junctions was measured in different solvent environments using a point contact technique based on a scanning tunneling microscope. It was shown that increasing the Au contact work function reduces the separation between the Au Fermi energy and the HOMO of BDA in the junction, thus increasing the measured conductance [23]. A detailed discussion of the questions of stability and conductivity of the molecular junctions are presented in [1, 10, 18]. Electron tunneling through a metal-molecule-metal junction is considered as a sequential process to explain the behavior of conduction through molecular contacts [24]. In the sequential tunneling model, the molecule is treated as a quantum dot with discrete energy levels weakly coupled to both electrodes through tunnel junctions. The molecule is successively charged and discharged. There are tunnel barriers at both ends of the molecule. The nitrogen species in 1,4 benzenediamine ($C_6H_8N_2$), chemically adsorbed on the gold electrodes, contributes to the HOMO and LUMO. As it is known electron-donating substituents, which drive the occupied molecular orbitals up, increase the junction conductance, while electron-withdrawing substituents have the opposite effect [18]. The behavior of the single BDA molecule bridging Au or Pt electrodes was also investigated in [25]. The conductance of molecular junctions with Au−NH_2 bonds was found to be equal to $1 \times 10^{-2}\, G_0$ (G_0 is the quantum conductance). Moreover, the stretching length of the molecular contacts Au–NH_2 was 0.03 nm. The conductance value of the Au−NH_2 molecular junction was unexpectedly larger than the value evaluated using the density of states of the metal electrodes and the molecule−metal bond strength. The large conductance value is explained by the small energy difference between metal and molecular orbitals and the high degree of π-conjugation of the Au−NH_2 molecular junction [25]. The results of our previous investigations on the current behavior and noise characteristics of gold-BDT (benzene-1,4-dithiol) molecule-gold junctions at room temperature and low bias voltages are presented in [20, 21, 26]. A Lorentzian-shape noise component was registered in addition to $1/f$-noise. The Lorentzian-type noise was interpreted as a manifestation of a dynamic reconfiguration of the molecular coupling to the metal electrodes [26]. The transport properties of bare gold and molecule-containing tunable Au-BDT-Au nanoconstrictions were studied using low-frequency noise spectroscopy in [21]. Models describing the noise behavior for bare gold and BDT-modified samples were developed and compared with the experimental data for three transport regimes: diffusive, ballistic and tunneling [21]. The transport mechanisms in metal–molecule–metal junctions after a break were analyzed in [20]. In [27] the process of formation of organometallic oligomer chains is analyzed using the MCBJ technique operated in a liquid environment. Alternating isocyanoterminated benzene monomers coordinated to gold atoms is considered. The behavior of quantum conductance versus relatively large displacement $G(\Delta d)$ at the opening and closing of the nanogap is investigated.

The temperature independent ballistic tunneling current for small molecules with a small vibrionic correction is discussed in [28, 29]. The correction was observed in the inelastic tunneling spectroscopy as a very small modulation of the slope in the current-voltage characteristic at the bias voltage corresponding to the molecular vibration energy. The problems of vibrations of a molecule in an external force field are demonstrated also in [30]. It is known that transition from ballistic transport to the hopping transport observed as a function of the molecular length and temperature for both self-assembled monolayers and single molecules is explained by the standard theory [31, 32]. In these scanning tunneling microscopy break junction experimental measurements, data are collected in the area of the conductance plateau. The question of the instability behavior (vibrations) of a conductance on a plateau remains almost open and should be explained.

The analysis of our experimental results here indicates that a new effect appears in molecular junctions, particularly at the transition from a diffusive to a ballistic regime or in the ballistic transport mode except of universal conductance fluctuations (UCF)[3]. This effect may cause weak instability in conductance in a narrow temperature range. It appears as local changes in quantum conductance in the order of quanta or smaller conditioned by small random changes in working regime (temperature, gap enlargement etc), resulting in some activation processes. On the basis of empirical data, we explain the unusual, observed conductance behavior for small changes in temperature and displacement for a gold-BDA-gold molecular junction. Since the quantum conductance is very sensitive to the energy structure of HOMO-LUMO, even weak effects impacting on the HOMO-LUMO can significantly affect the nature and behavior of the quantum conductance.

2. Experimental details

2.1. Fabrication procedure

We used MCBJs, fabricated at the Helmholtz Nanoelectronic Facility of Forschungszentrum Jülich GmbH, Germany, as experimental samples. The samples were fabricated from rectangular, flexible substrates made of stainless steel. The lateral dimensions were 12×55 mm and the thickness was 0.15 mm. Several layers of polyimide PI2561 were subsequently spin-coated onto the substrates to create an insulating layer. The samples were then covered with a stack of e-beam-sensitive polymers (polymethyl methacrylate PMMA 649.04 and PMMA 679.04). After e-beam patterning, metal deposition was used to create large contact pads and nanoconstrictions simultaneously. After the lift-off process and reactive ion etching, the samples were ready for measurements. More detailed information on the fabrication technology can be found in [33–35].

[3] UCF observed in mesoscopic conductors for which the phase coherence length is much longer than the sample size, while the elastic scattering length is much smaller than the size of the system [24].

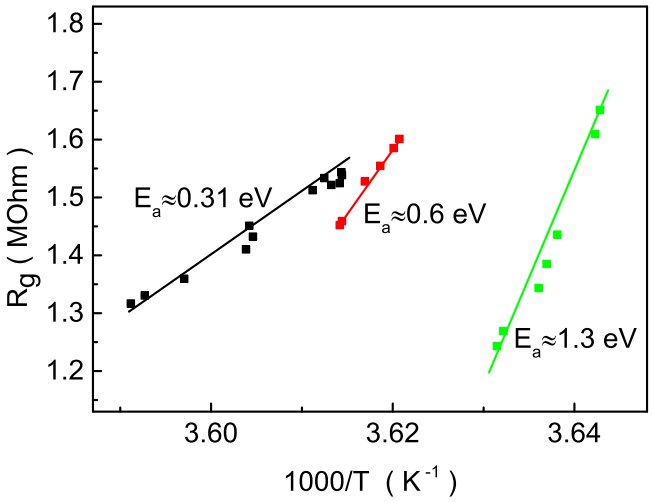

Figure 1. Gold-BDA-gold resistance R_g versus inverse temperature measured in the near-ballistic regime. E_a indicates the corresponding activation energies for the three processes of resistance change with decreasing temperature. A detailed description of these processes is given later in the text.

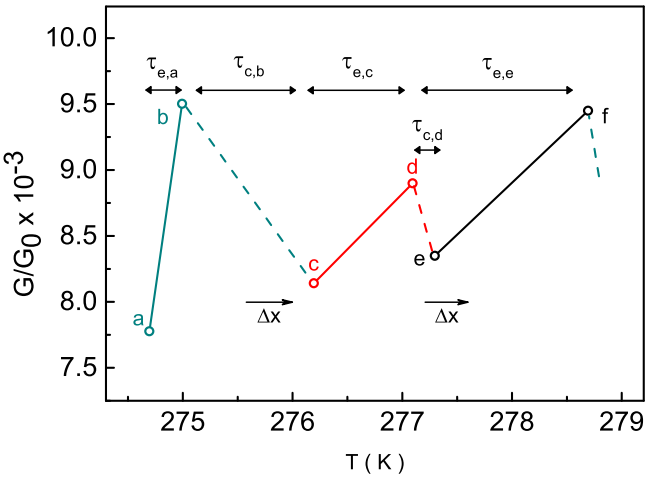

Figure 2. Dependence of thermal (kT) activation conductance on temperature for an Au-BDA-Au molecular junction plotted using $R_g(1/T)$ dependence (see figure 1). Through Δx we marked elementary change (growth) of the gap length between electrodes. Through τ_e and τ_c marked RTS emission and capture times for corresponding conduction states (see text below for details). The transitions from point 'a' to point 'b', 'c' to 'd' and 'e' to 'f' are marked with green, red and black dots in figure 1, respectively.

2.2. Resistance measurements of gold-BDA-gold molecular junctions

After fabrication, we introduced 10^{-6} M 1,4-benzenediamine solution in ethanol to the surface of our sample by drop casting. We used an immobilization time of several minutes, during which amino groups of the investigated molecule bond with the gold via covalent bonding. The excess of molecules that did not bind to the gold was later removed by rinsing in ethanol. To measure the electrical properties, we first bent our sample until the gold nanoconstriction on the top broke and a single BDA molecule bridged two electrodes (lock-in state). We obtained a resistance value of 1.2 MΩ for the system at room temperature, which agrees well with the literature data [25]. All measurements were performed in high vacuum ($\sim 10^{-6}$ mbar) in a shielded environment. After establishing the molecular junction, we measured the conductance at different temperatures in the range 274.5–278.7 K. This range is relatively narrow because even low temperature changes alter the stiffness of the gold and break the junction. To investigate the influence of mechanical strain on the electrical properties of the system, we altered the gap width by bending our sample. This resulted in a change of system resistance at room temperature. The dependence of the sample resistance on inverse temperature at different bending points is shown in figure 1. First of all we measured the resistance change of gold-BDA-gold molecular junction with decreasing of the temperature. When resistance increases due to MCBJ break we reduced distance between two electrodes and continue to measure the temperature dependence of resistance with definite position of molecule bridged two electrodes (red points in figure 1). At some temperature, resistance increases rapidly and distance between the contacts was again adjusted to attach the BDA molecule. In this configuration the temperature measurements (green points) were continued. The dependences R_g $(1/T)$ and data given in figure 1 are taken from a number of measurements. Each data point is obtained by the averaging of resistances, measured about 5 times with a step of two minutes at a certain temperature. The reproducibility of the data was confirmed by following experiment. After decreasing the temperature the behavior of the resistance dependence with increase of the temperature was obtained to be about the same within the experimental error. The most typical resistance dependence on temperature is used for the analysis.

3. Conductance analyses

Small fluctuations in the working temperature regime apply to all devices. For molecular junctions, this occurs when there is a certain gap between the metal electrodes. These fluctuations are random processes. Molecular junctions are much more sensitive to such influences than the more 'macroscopic' devices. To investigate the quantum conductance (G) behavior, even small changes in temperature and in the gap length between electrodes have to be taken into consideration. To physically explain the processes, it is more convenient to use the direct temperature gradient than the inverse temperature gradient. Therefore, we describe the processes using the inverse value of R_g, i.e. quantum conductance $G(T)$ instead of $R_g(1/T)$. Figure 2 shows the $G(T)$ dependence on temperature change in small intervals from 274.5 to 278.7 K with values taken from the experimental data for resistance $R_g(1/T)$ (see figure 1).

3.1. Description of the quantum conductance behavior (figure 2)

At a certain gap length, the conductance of the molecule corresponds to the state value $G_a \approx 7.8 \times 10^{-3}\, G_0$ (point 'a')

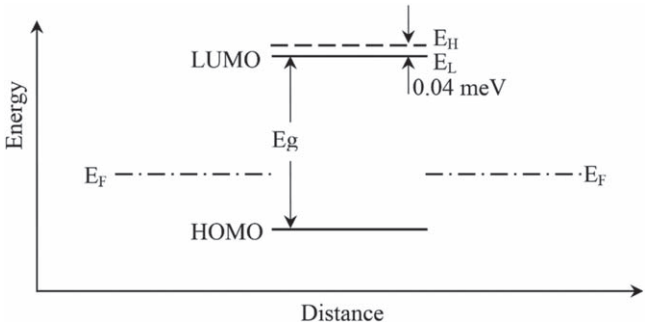

Figure 3. Schematic of the energy levels for a gold-BDA-gold junction at zero applied voltage. Here, the low-energy stable state is taken as the lowest unoccupied molecular orbital (LUMO) level. The excited energy level is presented as a sub-level E_H. Here, the HOMO is the highest occupied molecular orbital. E_F is the Fermi energy.

and the molecule is in a low-energy state E_L. Here, the quantum conductance is $G_0 = (12.9\,\mathrm{k\Omega})^{-1}$. Increasing the temperature by ~0.8 K molecule receives additional thermal energy ΔE and it is excited from a low energy level (point 'a') up to a higher excited energy level E_H (point 'b') and the conductance increases to $G_b \approx 9.5 \times 10^{-3} G_0$. This is described below in section 3.2 (see also figure 3). The temperature change of 0.8 K corresponds to the change in the thermal energy of the molecule $\Delta E = 0.04$ meV $= 6.4 \times 10^{-24}$ J. A simultaneous increase in the gap on Δx results in conductance modulation. The molecule quickly acquires additional thermal energy $\Delta E \approx 0.04$ meV to compensate the forces arising from the extension of the gap elementary length, from the molecule orientation and/or from position changes. Conductance again falls, dropping to a low value of $G_c \approx 8.1 \times 10^{-3} G_0$ (point 'c'). The molecule therefore returns to the low-energy stable state. Further temperature increases with the same temperature step of ~0.8 K and transfer energy ΔE causes the molecule to revert to a highly conducting metastable state E_H at point 'd' ($G_d \approx 8,9 \times 10^{-3} G_0$). Continuing increases in the gap length between the electrodes of the elementary magnitude Δx causes the molecule to return again to a low-conductance stable state E_L (point 'e', $G_e \approx 8,3 \times 10^{-2} G_0$). When the temperature increases further, the molecule moves to a high-energy state level E_H (point 'f', $G_f \approx 9,3 \times 10^{-3} G_0$). During all transitions from point 'a' to point 'b', 'c' to 'd' and 'e' to 'f', the change in conductance (modulation deepness) is not very large and is only (1.1–1.2 quanta). For comparison, stable contacts were observed in [36] with both low conductance in the order of 10^{-3} conductance quanta as well as with high conductance values above ~0.5 quanta. Our data unambiguously show that the conductance of the BDA molecule is determined by a single transport channel provided by the same molecular level, which is coupled to the metallic electrodes through the whole conductance range.

Each transition process from low to high energy levels 'a'–'b', 'c'–'d' and 'e'–'f' is accompanied by the characteristic activation energy E_a (see figure 1), calculated according to following relationship:

$$R(T) = \mathrm{Const} \times \exp\left(-\frac{E_a}{kT}\right). \quad (1)$$

We used experimental data from figure 1. For the transitions, the following activation energy values were calculated: for 'a'–'b' $E_{a,a-b} \approx 2.1 \times 10^{-19}\,J = 1.3$ eV; for 'c'–'d' $E_{a,c-d} \approx 0.96 \times 10^{-19}\,J = 0.6$ eV; and for 'e'–'f' $E_{a,e-f} \approx 0.5 \times 10^{-19}\,J = 0.31$ eV. It should be noted that the energy is reduced almost twofold for each step. These experimental data will be explained below.

3.2. Analyses of the experimental data

It is quite clear that observed and presented above effect of the quantum conductance modulation. At the transitions from states 'b' to 'c' and 'd' to 'e', the conductance decreases with an increasing gap on Δx. Similar behavior of the quantum conductance amplitude at 4.2 K was also observed in [37]. Features of these transitions will be discussed later. For a visual understanding of the molecule conductance (energy) temperature modulation process, figure 3 presents a schematic of the energy levels for a gold-BDA-gold junction. The low-conductance stable energy state is taken as the LUMO level, and the level with energy E_H corresponds to the excited state.

The behavior of the currents through the junction was considered. The presented results (basic data in figure 1) were obtained after bond breaking in the junction. Under a low applied voltage ($V < \Phi/e$, Φ is the metal work function) through the junction, a direct tunnel current flows (see also [20]). The current values corresponding to high-conductance and low-conductance states at the applied voltage 20 mV were calculated as[4]:

$$I_H = G_H V = G_b V \approx 9.5 \times 10^{-3} G_0 V \approx 14.7\ \mathrm{nA}.$$
$$I_L = G_L V = G_a V \approx 7.8 \times 10^{-3} G_0 V \approx 12.1\ \mathrm{nA}.$$

The average current was calculated as:

$$I_{av} = \frac{I_H + I_L}{2} = 13.4\ \mathrm{nA}.$$

The high and low current states differ by 2.6 nA and the maximum magnitude of the conductance modulation is equal to $(G_{\max} - G_{\min})/G_{\max} \approx (G_b - G_a)/G_b \approx 0.18$, or 18%.

For further analysis, we used information obtained from random telegraph signal (RTS) measurements on gold-BDT (benzene-1,4-dithiol)-gold junctions in [38] (see figure 3 in [38] and its description). A small RTS signal was registered, and the difference between the high and low current states was about $\Delta I \approx 1.5$ nA at an average current $I \approx 14$ nA with current fluctuations below 12%. In our experiment, the average current, I, was also used at a level of ≈14 nA. The conductance modulation effect was small for the BDA molecule and BDT molecules. We assume that the quantum conductance weak modulation discussed above directly affects the RTS behavior. In this case such, the emission and

[4] Measurements of resistance as a function of temperature were performed at an applied voltage of 20 mV and are shown in figure 1 as dependence on the inverse temperature.

capture times τ_e and τ_c in the RTS process can be described as follows. Capture time is the time during which the molecule is in the low-conductance steady state corresponds to the LUMO energy level (E_L level). This corresponds to low-conductance states (points 'a', 'c' and 'e'). During the emission time, the molecule moves in an 'excited' metastable state E_H (see figure 3), and conductance and therefore current increase (states 'b', 'd' and 'f'). The conduction modulation value is ∼18% and the depth of the current modulation is ∼12%. The difference in modulation depths in these processes is not large. It should be also noted that a relatively low value of the conduction modulation deepness (18%) can be associated with small changes in temperature. For comparison, in nanotubes, giant RTS values of 60% [37] or more than 80% [2] have been reported.

The regular recurrence of the conductance in each temperature step of 0.8 K has to be conditioned by the BDA molecule 'energy gap construction' peculiarities. We assume that the BDA molecule has a sub-band near LUMO with an energy corresponding to (0.04 eV). The conductance activation energy E_a also decreases approximately twice during each temperature increase of 0.8 K (1.3 eV, 0.6 eV and 0.31 eV, respectively). Such regularity in quantum conductance and activation energy changes could be related to physical and mechanical effects and can be used to characterize the molecular junction with a BDA molecule. Assuming that there are some regularly distributed energy barriers, it is clear that with increasing temperature such barriers can be more easily overcome and the effective E_a decreases. In such a case, there are quasi-levels regularly distributed in energy between HOMO and LUMO, and activation processes can be performed through those levels. The higher the temperature, the easier the electron transition from a stable state to a metastable state. However, if the electric field is high, the hot electrons may also overcome the barrier. In our case where the applied voltage is 20 mV, the resulting electric field in the junction is small (of the order of 10^4–10^5 V cm^{-1}), which reflects that the effect of hot electrons can be neglected.

The results in [39] show that increasing the molecular length results in a decrease in the HOMO-LUMO gap, a decrease in the electrical conductance and an increase in the value and oscillation of the thermo-power, reflecting thermo-activation processes in the structure. The RTS was observed during break junction experiments with gold binding molecules in [40]. The authors attributed the emergence of signals to the spontaneous binding and unbinding of the molecular anchor groups to and from the electrode tips. Both the formation and the breaking of the molecule–metal bonds are thermally activated and show an exponential distribution of lifetimes for the different conductance states. The difference in RTS amplitudes as well as in capture and emission times is associated with different microscopic conduction mechanisms. The large RTS amplitude observed in [40] is related to a total break between the molecule and metal contact. In our work, in contrast to [40], we studied transport phenomena with only a small configurational change in the contact with no break or disconnection between the molecule and metal.

It should be noted, that in opposite to the case considered in [27] in our measurements we demonstrate the dependence of quantum conductance versus displacement $G(\Delta x)$ only at the gap opening and the simultaneous action of slow temperature activation. Our measurements also show that magnitude of G decreases with the increase of displacement (from point 'b' to 'c', 'd' to 'e', figure 2), but the process occurs with weak thermal activation (from point 'a' to 'b', 'c' to 'd'). With the growth of Δx, we do not see a plateau in the dependence $G(\Delta d)$, (see e.g. figure 1(c) [27]) because Δx is much smaller and it does not reach the formation of a plateau. As we can see in figure 2(b) [27] the decreasing of G with Δd accompanied by plots of local growth of G (for example, between points 1 and 2, or points 3, 4, 5, figure 2(b) [27]). In the figure 1(c) and figure 3(a) in [27] on the plateau of the dependency $G(\Delta d)$, nanoscale fluctuations of conductance are clearly visible. These fluctuations are probably also the result of some activation processes. Note also that these nanoscale fluctuations occur at distances of the order of 0.1 nm (figure 3(a) [27]), which is a comparable value with our Δx value. When we change the gap size on Δx, we also have nanoscale fluctuations of conductance, which we explained by thermal activation processes.

Conductance (resistance) thermo-sensitivity S_{TG} (or S_{TR}) of the molecule can be presented as the change in conductance ΔG (resistivity ΔR) at the temperature change in ΔT:

$$S_{TG} = \frac{\Delta G}{\Delta T},\ S_{TR} = \frac{\Delta R}{\Delta T}. \tag{2}$$

Based on the data in figures 1 and 2 for the BDA molecule, we get $S_{TG} \approx (0.8 \div 1.6) \times 10^{-7}\ \Omega\ \mathrm{K}^{-1}$ ($S_{TR} \approx (2.5 \div 5) \times 10^5\ \Omega\ \mathrm{K}^{-1}$). This reflects sufficiently high sensitivity.

The molecule with additional energy has to lose it on some processes. The additional energy $\Delta E = 6.4 \times 10^{-24}$ J (corresponding to a temperature change of 0.8 K) is much smaller than the potential energy. Assuming that the molecule with additional energy ΔE spends this additional energy to compensate for the force F arising from the elongation of the gap length[5], then

$$\Delta E = F\Delta x. \tag{3}$$

For example, in the case of a one-dimensional elastic force in linear approximation, we use Hooke's law:

$$F_H = |k_s \Delta x|,\ \ \Delta E \equiv k_B T = k_s (\Delta x)^2,\ k_s = \frac{\Delta E}{(\Delta x)^2}. \tag{4}$$

Here, k_s is the molecular spring constant, k_B is the Boltzmann constant. The stretching length of the Au−NH_2 molecular junction was 0.03 nm [25]. Assuming that the elementary

[5] It is also possible that this additional energy will be spent on the molecule orientation or position change or on the formation and breaking of molecule–metal bonds, as noted in [28]. A change in configuration can be effected on the molecular level ($E_F - E_{HOMO}$) position and level broadening [36].

enlargement is equal to stretching length $\Delta x = 0.03$ nm, then

$$k_s = \frac{\Delta E}{(\Delta x)^2} = \frac{4 \times 10^{-5}}{(0.03 \times 10^{-9})^2}\ \text{eV m}^{-2} = 7.1 \times 10^{-3}\ \text{N m}^{-1}. \tag{5}$$

According to experimental and theoretical results presented in [19] for Au-BDA-Au molecular junctions, the rupture force $F_{\text{rupt}} = 0.4$ nN (expt), $F_{\max} = 1.0$ nN (expt fit), $L_{\text{bind}} = 1.4$ Å (expt fit), $L_{\max} = 0.46$ nN (theory), $L_{\text{bind}} = 1.09$ Å (theory), $E_{\text{bind}} = 0.37$ eV (theory). Here F_{rupt} is the Au−N rupture force and bond strength, $F_{\max}$ is the maximum sustainable force, E_{bind} is the metal/molecule binding energy, L_{bind} is the binding distance.

In our case, $k_s = 7.1 \times 10^{-3}\ \text{N m}^{-1}$ and $\Delta x = 0.03$ nm. Using equation (4), we obtained $F_H = 0.00021$ nN. This is 3 orders of magnitude smaller than the rupture force in [19]. This confirms that there is no breaking in our case.

For comparison, we will consider the case when expansion forces are compensated by Coulomb forces F_C. For simplicity, we assume that the ends of the molecule are singly ionized (effect of monovalent gold atoms). Then, instead of equation (3), we get

$$F_C = F,\ \frac{k_e e^2}{(l_m + \Delta x)^2} = k_C \Delta x. \tag{6}$$

Here, BDA molecule length is $l_m \approx 0.57$ nm, and $k_e = 8.99 \times 10^9\ \text{N m}^2\ \text{C}^{-2}$ is Coulomb's constant. At $\Delta x = 0.03$ nm, $k_C = 21.31\ \text{N m}^{-1}$. Comparison of magnitudes for k_s and k_C shows that the forces arising due to the activation energies are hundreds of times weaker than electrostatic forces. The forces arising due to the activation energies cannot significantly influence the current transport processes, but can affect the strength of the electrode-molecule coupling, the fluctuation of quantum conductivity and hence the RTS behavior. This result is in good agreement with the assumption that different bond states influence the strength of the electrode-molecule coupling at the tilt angle of the molecule and the binding of the end group on the top or hollow site, which is also referred to in [36]. Another study [41] also showed that the energetic position of the molecular orbital may determine the transmission conductivity.

4. Conclusion

We presented and analyzed the electric and enlargement-specific characteristics of gold-BDA-gold molecular junctions. The nanoconstriction junctions were fabricated using electron beam lithography. We performed and analyzed measurements of quantum resistance dependence on small changes in temperature and displacement. We revealed the relationship between the small changes in quantum conductance and RTS behavior. We showed that RTS measurements (determination of the capture and emission times, deepness of the current modulation, values of the minimum and maximum currents) can help us understand quantum conductance modulation processes and clarify the mechanisms of acquiring and losing additional thermal energy during average current flow in a gold-BDT-gold molecular junction. We showed that small changes in working temperature led to a change in quantum conductance, which was reflected in the RTS behavior. On the basis of RTS measurements, we revealed energy sublevels of the BDA molecular orbitals (LUMO, HOMO) and peculiarities of HOMO-LUMO gap, in particular the broadening and narrowing of the gap, the energy position of the excited state and regularly distributed levels in the gap. Using capture and emission times from RTS measurements, we determined the mechanisms and kinetics of the change in conductance. We propose that RTS measurements and the determination of the high and low current states can be utilized to determine changes in conductance under external influences, such as temperature or irradiation. We registered a high sensitivity of the molecules to small changes in temperature. For the BDA molecule, the conductance thermo-sensitivity is relatively high equal to $(0.8 \div 1.6) \times 10^{-7}\ (\Omega\text{K})^{-1}$. This can be used to measure weak variations in the ambient temperature. We showed that the additional thermal energy produced by the change in temperature can affect the strength of the electrode-molecule coupling, the fluctuation of quantum conductance and hence the RTS behavior. We demonstrated a new approach on the basis of conductance modulation to define the spring constant. We determined the value of this spring constant for the BDA molecule at the stretching length of the Au−NH_2 molecular junction (0.03 nm) as $k_s = 7.1 \times 10^{-3}\ \text{N m}^{-1}$. These results can be used to develop devices for molecular electronics.

Acknowledgments

F Gasparyan greatly appreciates support in the form of a research grant from the German Academic Exchange Service (DAAD). The authors would like to thank V Sydoruk for his preliminary work.

ORCID iDs

S Vitusevich https://orcid.org/0000-0003-3968-0149

References

[1] Agraït N, Yeyati A L and van Ruitenbeek J M 2003 *Phys. Rep.* **377** 81–279
[2] Wang N-P, Heinze S and Tersoff J 2007 *Nano Lett.* **7** 910–3
[3] de M Souza A *et al* 2014 *Nanoscale* **6** 14495–507
[4] Martin C A, Ding D, van der Zant H S J and van Ruitenbeek J M 2008 *New J. Phys.* **10** 065008
[5] Van Ruitenbeek J M, Alvarez A, Pineyro I, Grahmann C, Joyez P, Devoret M H, Estéve D and Urbina C 1996 *Rev. Sci. Instrum.* **67** 108–11
[6] Fujihira M, Suzuki M, Fujii S and Nishikawa A 2006 *Phys. Chem. Chem. Phys.* **8** 3876–84
[7] Datta S, Tian W, Hong S, Reifenberger R, Henderson J I and Kubiak C P 1997 *Phys. Rev. Lett.* **79** 2530
[8] Tao N J 2006 *Nat. Nanotechnol.* **1** 173–81

[9] Wang C-K, Fuc Y and Luo Y 2001 *Phys. Chem. Chem. Phys.* **3** 5017–23
[10] Na J-S, Ayres J, Chandra K L, Chu C, Gorman C B and Parsons G N 2007 *Nanotechnology* **18** 035203
[11] Nitzan A and Ratner M A 2003 *Science* **300** 1384–9
[12] Cui X D, Zarate X, Tomfohr J, Sankey O F, Primak A, Moore A L, Moore T A, Gust D, Harris G and Lindsay S M 2002 *Nanotechnology* **13** 5–14
[13] Selzer Y, Salomon A and Cahen D 2002 *J. Phys. Chem.* B **106** 10432–9
[14] Selzer Y, Cai L, Cabassi M A, Yao Y, Tour J M, Mayer T S and Allara D L 2005 *Nano Lett.* **5** 61–5
[15] Datta S 2004 *Nanotechnology* **15** S433–51
[16] McCreery R 2004 *Chem. Mater.* **16** 4477–96
[17] Troisi A and Ratner M 2006 *Small* **2** 172–81
[18] Venkataraman L, Park Y S, Whalley A C, Nuckolls C, Hybertsen M S and Steigerwald M L 2007 *Nano Lett.* **7** 502–6
[19] Hybertsen M S and Venkataraman L 2016 *Acc. Chem. Res.* **49** 452–60
[20] Gasparyan F 2017 *J. Contemporary Phys.* **52** 121–8
[21] Handziuk V, Gasparyan F, Vandamme L K J, Coppola M, Sydoruk V, Petrychuk M, Mayer D and Vitusevich S 2018 *Nanotechnology* **29** 385704
[22] Tobita J, Kato Y and Fujihira M 2008 *Ultramicroscopy* **108** 1040–4
[23] Fatemi V, Kamenetska M, Neaton J B and Venkataraman L 2011 *Nano Lett.* **11** 1988–92
[24] Porath D, Levi Y, Tarabiah M and Millo O 1997 *Phys. Rev.* B **56** 9829–33
[25] Kiguchi M, Miura S, Takahashi T and Murakoshi K 2008 *J. Phys. Chem.* C **112** 13349–52
[26] Sydoruk V A, Xiang D, Vitusevich S A, Petrychuk M V, Vladyka A, Zhang Y, Offenhäusser A, Kochelap V A, Belyaev A E and Mayer D 2012 *J. Appl. Phys.* **112** 014908
[27] Vladyka A, Perrin M L, Overbeck J, Ferradás R R, García-Suárez V, Gantenbein M, Brunner J, Mayor M, Ferrer J and Calame M 2019 *Nat. Commun.* **10** 262
[28] Okabayashi N, Paulsson M, Ueba H, Konda Y and Komeda T 2010 *Nano Lett.* **10** 2950–5
[29] Hihath J and Tao N 2012 *Prog. Surf. Sci.* **87** 189–208
[30] Okabayashi N, Peronio A, Paulsson M, Arai T and Giessibl F J 2018 *Proc. Natl Acad. Sci. USA* **115** 4571–6
[31] Choi S-H, Kim B S and Frisbe C D 2008 *Science* **320** 1482–6
[32] Lee S-K, Yamada R, Tanaka S, Chang G S, Asai Y and Tada H 2012 *ACS Nano* **6** 5078–82
[33] Handziuk V, Coppola M, Gasparyan F, Sydoruk V, Mayer D and Vitusevich S *Proc. 24th Int. Conf. on Noise and Fluctuations (Vilnius, Lithuania, 20–23 June 2017)* pp 19–22
[34] Xiang D, Jeong H, Lee T and Mayer D 2013 Mechanically controllable break junctions for molecular electronics *Adv. Mater.* **25** 4845–67
[35] Wang L, Wang L, Zhang L and Xiang D 2017 Advance of mechanically controllable break junction for molecular electronics *Top. Curr. Chem.* **375** 61
[36] Kim Y, Pietsch T, Erbe A, Belzig W and Scheer E 2011 *Nano Lett.* **11** 3734–8
[37] Liu F, Bao M, Kim H, Wang K L, Li C, Liu X and Zhou C 2005 *Appl. Phys. Lett.* **86** 163102
[38] Xiang D, Sydoruk V, Vitusevich S, Petrychuk M V, Offenhausser A, Kochelap V A, Belyaev A E and Mayer D 2015 *Appl. Phys. Lett.* **106** 063702
[39] Golsanamlou Z, Vishkayi S I, Tagani M B and Soleimani H R 2014 *Chem. Phys. Lett.* **594** 51–7
[40] Brunner J, González M T, Schönenberger C and Calame M 2014 *J. Phys. Condens. Matter* **26** 474202
[41] Briechle B M, Kim Y, Ehrenreich P, Erbe A, Sysoiev D, Huhn T, Groth U and Scheer E 2012 *Beilstein J. Nanotechnol.* **3** 798–808